mathematics

MDPI

Article

Simultaneous Tracking and Stabilization of Nonholonomic Wheeled Mobile Robots under Constrained Velocity and Torque

Yuan Li [1], Yuyang Cai [1], Yong Wang [1], Wei Li [2,*] and Gang Wang [1]

[1] School of Health Science and Engineering, University of Shanghai for Science and Technology, Shanghai 200093, China
[2] School of Finance, Shanghai Lixin University of Accounting and Finance, Shanghai 201209, China
* Correspondence: li_wei@lixin.edu.cn

Abstract: Currently, most assumptions in nonholonomic mobile robot controllers indicate that the robot velocity can become significantly large and that the robot actuators are able to generate the necessary level of torque input. Based on the sliding mode control theory, this paper develops a new framework to handle the control problem of a wheeled robot dynamics model with constrained velocity and torque. Through rigorous theoretical analysis and extensive simulations, we demonstrate that the proposed controller guarantees asymptotic convergence of tracking or stabilization errors and boundedness of closed-loop signals. The advantages of the developed controller include the ability to simultaneously achieve tracking and stabilization control of nonholonomic mobile robots and the ability to ensure that the prescribed velocity and torque constraints are not breached by simply tuning the design parameters a priori, even in the presence of uncertain disturbances.

Keywords: sliding mode control; adaptive control; trajectory tracking; Lyapunov design; mobile robot

MSC: 93D50

check for updates

Citation: Li, Y.; Cai, Y.; Wang, Y.; Li, W.; Wang, G. Simultaneous Tracking and Stabilization of Nonholonomic Wheeled Mobile Robots under Constrained Velocity and Torque. *Mathematics* **2024**, *12*, 1985. https://doi.org/10.3390/math12131985

Academic Editors: Anatoliy Swishchuk and Daniel-Ioan Curiac

Received: 23 May 2024
Revised: 20 June 2024
Accepted: 25 June 2024
Published: 27 June 2024

Copyright: © 2024 by the authors. Licensee MDPI, Basel, Switzerland. This article is an open access article distributed under the terms and conditions of the Creative Commons Attribution (CC BY) license (https://creativecommons.org/licenses/by/4.0/).

1. Introduction

The investigation of nonholonomic systems is an intriguing topic to which numerous research efforts have been devoted over the past three decades [1]. The appeal of nonholonomic systems comprises the wide range of potential applications of these systems and the corresponding technical challenge, namely, the absence of continuous time-invariant stable controllers for these systems, inferred from the well-known Brockett's theorem. Many significant strategies have been presented for the stabilization problem of nonholonomic systems, such as smooth time-varying feedback [2], output feedback control [3], predefined-time stability [4], and switching-based state-scaling design [5]. In addition to stabilization control, the interesting tracking control problem of nonholonomic mobile robots has also been comprehensively investigated using the dynamic feedback linearization method [6], backstepping technique [7], dynamic feedback control [8], sliding mode control [9], fixed-time control [10], predefined-time control [11], and model predictive control [12]. Recently, by applying attitude observers, the trajectory tracking problem for nonholonomic mobile robots was solved using only Cartesian position and velocity measurements in [13,14]. Different from the aforementioned approaches that are only applicable to either stabilization or tracking control for mobile robots, a unified control algorithm that can address both stabilization and tracking issues was designed in [15–18]. Nevertheless, these works focus on the canonical control issue while disregarding the practical limitations of robotics.

For real-world applications, the limitations on nonholonomic mobile robots emerge as saturation constraints of the motor torque and velocity constraints imposed for safety specifications. By using passivity and normalization, Ref. [19] presented two feedback laws for addressing stabilization and tracking control, respectively, for a wheeled mobile

robot with input saturations. Using sliding mode control, the semiglobal stabilizability of nonholonomic robots with saturated inputs was considered in [20]. By applying the nested saturation technique and switching the control design strategy, finite-time stabilization for a class of nonholonomic feedforward systems was addressed in [21]. The tracking control of mobile robots with diamond-shaped input constraints was explored in [22] to better exploit the tracking ability of the robots. The tracking control of mobile robots with bounded velocities and torques was considered in [23]. A control method for trajectory tracking of nonholonomic robots with angular velocity saturation and bounded linear velocity with a positive-minimum value was designed in [24]. Recently, an adaptive trajectory tracking control scheme for low-speed, car-like vehicles with input constraints was presented in [25]. The above works indicate that the proposed controllers for trajectory tracking and stabilization are individually designed [7,20–24] and have to be switched according to the specific application. To address the problem of simultaneous stabilization and tracking, a backstepping-based controller was designed for a class of unicycle-modeled mobile robots with saturation constraints in [26,27]. Nevertheless, the results were obtained under somewhat conservative requirements: the reference linear velocity of the robots was required to be nonnegative. In [28], adaptive stabilization and tracking control of a nonholonomic mobile robot with torque saturation were separately considered. Recently, the control problems of tracking and stabilization simultaneously for mobile robots with input constraints were investigated by applying radial basis function approximations and projection-type adaptation laws in [29]. However, the velocity constraints were not explicitly considered.

The current work aims to address the problem of designing a unified tracking and stabilization control controller for a nonholonomic mobile robot with both velocity constraints and torque constraints in the presence of model uncertainty. This research significantly complements the results in [26–29], where no velocity constraint was imposed on the robot. Theoretical and simulation verifications of the controller guaranteeing asymptotic convergence of tracking or stabilization errors and the boundedness of each signal in the closed-loop system are carefully analyzed. Compared with the existing works, the main contribution of this paper lies in three aspects:

(i) In addition to torque constraints, significant velocity constraints are taken into account for safety reasons. Furthermore, for any positive constraints on the velocity and control torque, the design parameter can be simply determined *a priori* to prevent constraint violations.
(ii) In contrast with the results from separately designing two controllers for the stabilization and tracking tasks of a wheeled mobile robot, a unified time-varying controller that can actively compensate for unknown disturbances in the dynamic model is presented, possessing some distinct advantages, such as only one controller and improved transients because of no switching.
(iii) A more general mobile robot including both input constraints and uncertain disturbances is considered, and a new time-varying signal is tailored to handle these constraints at the dynamic level.

The remainder of this article provides the problem formulation in Section 2. Section 3 illustrates the controller design and stability analysis for mobile robots. Section 4 presents the simulation results for the stabilization task and tracking control task, while Section 5 establishes the conclusions.

Notation: For the vector function $f(t)$, we say that $f \in \mathcal{L}_\infty$ if $\sup_{0\le t<\infty} \|f(t)\| < \infty$ and that $f \in \mathcal{L}_p$ if $(\int_0^\infty \|f(t)\|^p dt)^{\frac{1}{p}} < \infty$. The limit $\lim_{t\to\infty} x(t) = a$ is abbreviated by $x \to a$.

2. Control Problem Formulation of Nonholonomic Mobile Robots

The dynamic model of the two-wheeled mobile robot is given as follows:

$$\begin{array}{rcl} \dot{x} & = & v\cos\theta \\ \dot{y} & = & v\sin\theta \\ \dot{\theta} & = & \omega \\ \dot{v} & = & \tau_1 + d_1 \\ \dot{\omega} & = & \tau_2 + d_2 \end{array} \tag{1}$$

where (x, y) denote the Cartesian coordinates; θ is the orientation; v and ω are the linear velocity and angular velocity, respectively; $d_1(t)$ and $d_2(t)$ may be taken as uncertain disturbances, including unmodeled dynamics; and τ_1 and τ_2 are the control torques of the robot. For safety specifications and physical limitations inherent to the motor, both the velocities and control torques need to satisfy the following constraints:

$$|v(t)| \le \phi_1, |\omega(t)| \le \phi_2, |\tau_1(t)| \le \varpi_1, |\tau_2(t)| \le \varpi_2, \forall t \ge 0 \tag{2}$$

where ϕ_1, ϕ_2, ϖ_1, and ϖ_2 are given arbitrary positive constants. The initial velocities and control torques are assumed to satisfy the above constraints.

The feasible reference trajectory is generated by the following virtual robot:

$$\begin{array}{rcl} \dot{x}_d & = & v_d\cos\theta_d \\ \dot{y}_d & = & v_d\sin\theta_d \\ \dot{\theta}_d & = & \omega_d \end{array} \tag{3}$$

where (x_d, y_d) and θ_d are the Cartesian coordinates and orientation, respectively, of the virtual robot, and v_d and ω_d are the linear velocity and angular velocity, respectively, of the virtual robot.

Remark 1. *Note that the two-wheeled mobile robot can be classified as a differential flat system. Thus, we can choose the flat outputs (x_d, y_d), and the desired orientation, linear velocity, and angular velocity can be expressed as [30]*

$$\begin{array}{rcl} \theta_d & = & \arctan(\frac{\dot{y}_d}{\dot{x}_d}) \\ v_d & = & \sqrt{\dot{x}_d^2 + \dot{y}_d^2} \\ \omega_d & = & \frac{\dot{y}_d\dot{x}_d - \ddot{x}_d\dot{y}_d}{\dot{x}_d^2 + \dot{y}_d^2}. \end{array}$$

This modification will help simplify the problem with both velocity and torque constraints. However, potential singularities should be considered when $v_d = 0$.

We interpret the tracking errors as

$$\begin{bmatrix} x_e \\ y_e \\ \theta_e \end{bmatrix} = \begin{bmatrix} \cos\theta & \sin\theta & 0 \\ -\sin\theta & \cos\theta & 0 \\ 0 & 0 & 1 \end{bmatrix} \begin{bmatrix} x - x_d \\ y - y_d \\ \theta - \theta_d \end{bmatrix} \tag{4}$$

whose derivative along (1) and (3) satisfies

$$\begin{array}{rcl} \dot{x}_e & = & -v_d\cos\theta_e + v + \omega y_e \\ \dot{y}_e & = & v_d\sin\theta_e - \omega x_e \\ \dot{\theta}_e & = & \omega - \omega_d. \end{array} \tag{5}$$

It can be verified that the asymptotic convergence of x_e, y_e, θ_e implies that of $(x - x_d)$, $y - y_d$, and $(\theta - \theta_d)$. In this paper, we consider reference trajectories (3) generated by a virtual nonholonomic mobile robot. Such a requirement is reasonable because it is difficult

for an underactuated robot to accurately track trajectories that exceed its maneuvering capabilities. There are also some tracking control methods that can achieve arbitrary reference trajectories using the transverse function approach [31]. However, only practical convergence of the tracking errors can be obtained.

The control objective is to design control torques τ_1 and τ_2, such that the position and orientation (x, y, and θ) of the mobile robot (1) can globally asymptotically track x_d, y_d and θ_d generated by (3), in the sense that

$$x_e(t) \to 0, y_e(t) \to 0, \theta_e(t) \to 2N\pi \tag{6}$$

while ensuring that the velocity and torque constraints defined in (2) are not transgressed, where N is an integer; refer to Figure 1. To achieve this goal, the following assumptions are created.

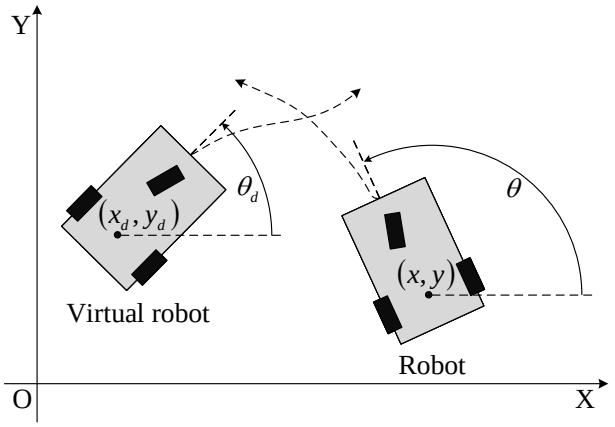


Figure 1. Trajectory tracking configuration of a two-wheeled nonholonomic mobile robot.

Assumption 1. *The uncertain disturbances d_1 and d_2 are bounded, i.e., $|d_1(t)| \leq \varsigma_1$ and $|d_2(t)| \leq \varsigma_2$ for all $t \geq 0$.*

Assumption 2. *The virtual robot is subject to velocity and torque constraints, that is, $|v_d(t)| \leq \mu_1 < \phi_1$, $|\omega_d(t)| \leq \mu_2 < \phi_2$, $|\dot{v}_d(t)| \leq \kappa_1 < \varpi_1 - \varsigma_1$, and $|\dot{\omega}_d(t)| \leq \kappa_2 < \varpi_2 - \varsigma_2$, where μ_1, μ_2, κ_1, and κ_2 are positive constants.*

Assumption 3. *The virtual robot needs to satisfy one of the following two conditions:*

$$\begin{array}{ll} \text{case C1}: & \int_0^\infty (v_d^2(\sigma) + \omega_d^2(\sigma))d\sigma \leq \varepsilon_1, \int_0^\infty |v_d(\sigma)|d\sigma \leq \varepsilon_2 \\ \text{case C2}: & \int_t^{t+\varepsilon_3} (v_d^2(\sigma) + \omega_d^2(\sigma))d\sigma \geq \varepsilon_4, \forall t \geq 0 \end{array}$$

where ε_1 and ε_2 are nonnegative constants and ε_3 and ε_4 are strictly positive constants.

The following result will be useful in the text.

Lemma 1 ([7]). *Consider a scalar system $\dot{x} = -kx + f(t)$, where $k > 0$ and $f(t)$ are bounded and uniformly continuous. If $x \in \mathcal{L}_\infty$ and $x \to 0$, then $\dot{x}, f \to 0$.*

Lemma 2 ([32]). *If the differentiable function $x(t)$ has a finite limit as $t \to \infty$ and if $\dot{x}$ is uniformly continuous, then $\dot{x} \to 0$.*

Remark 2. *Stabilization and tracking control of nonholonomic robots have been successfully implemented in various real-world scenarios. For example, in warehouse environments, autonomous mobile robots navigate to specific locations to pick up and place goods. These robots utilize stabilization and tracking control to follow predefined paths, avoid obstacles, and ensure precise positioning.*

Similarly, self-driving cars rely on advanced control systems for stabilization and tracking to navigate roads safely. In precision agriculture, autonomous tractors and harvesters employ precise stabilization and tracking control for planting, weeding, and harvesting tasks. These examples highlight the practical application and validation of the proposed method in diverse fields.

Remark 3. *Note that the stabilization problem of the mobile robot belongs to case C1 in Assumption 3, while the tracking problem belongs to case C2. Similar conditions can also be found in [16,17]. The importance of this property includes the requirement of only one unified controller, and as there is no switching, there is an improved transient performance compared with the use of separate stabilization and tracking control strategies [19,20,23]. Furthermore, separate stabilization and tracking control approaches will not work if the switching time is not available.*

Remark 4. *In this paper, we do not explicitly address obstacles and real-world assumptions. Instead, we adopt a feasible reference trajectory (3) that considers these factors to facilitate controller design and stability analysis. For practical applications, integrating path planning algorithms with artificial potential fields for nonholonomic mobile robots using our proposed method may address obstacle detection and avoidance. While this research is beyond the scope of this paper, it represents a promising area for future exploration.*

3. Simultaneous Tracking and Stabilization Controller Design and Tracking Error Convergence Analysis

Novel Time-Varying Signal: In [17,18], by introducing a time-varying signal to redefine the orientation error, a unified controller that can adaptively and smoothly transition between stabilizer and tracker rather than switch between these two different types of controllers was presented for mobile robots at the kinematic level. Inspired by [17,18], we tailor a novel time-varying signal $\xi = \eta f$ to solve the tracking and stabilization problems of mobile robots at the dynamic level while ensuring the satisfaction of the velocity and torque constraints. Here,

$$f = \rho \tanh(\sqrt{1 + x_e^2 + y_e^2} - 1) \sin t$$

$\dot{\eta} = -(v_d^2 + \omega_d^2)\eta$ with $\eta(0) = 1$, and ρ is a positive constant to be designed. One easily verifies $0 \leq \eta(t) \leq 1$ and $|\xi(t)| \leq |f(t)| \leq \rho$. The time-varying signal ξ differs from those in [17,18] in two aspects. First, unlike the signal in [17] that is only first-order differentiable, ξ in this work is second-order differentiable. This property enables it to be applied to control law design for nonholonomic mobile robots at the dynamics level. Second, as demonstrated in the following analysis, the first and second derivatives of ξ are bounded a priori, allowing for addressing velocity and torque constraints.

Kinematic Control Design: Design the virtual controllers α_v and α_ω as

$$\begin{array}{rcl} \alpha_v & = & v_d \cos \xi - \zeta_1 \\ \alpha_\omega & = & \dot{\xi} + \omega_d - \frac{\lambda v_d}{\sqrt{1+x_e^2+y_e^2}} (x_e \sin \frac{\theta_e + \xi}{2} + y_e \cos \frac{\theta_e + \xi}{2}) - \zeta_2 \end{array} \tag{7}$$

where λ is a positive constant. The update laws of ζ_1 and ζ_2 are designed as

$$\begin{array}{rcl} \dot{\zeta}_1 & = & \frac{l_1}{2} (\frac{x_e}{\sqrt{1+x_e^2+y_e^2}} - \frac{\zeta_1}{m_1}) \\ \dot{\zeta}_2 & = & \frac{l_2}{2} (\sin \frac{\theta_e - \xi}{2} - \frac{\zeta_2}{m_2}) \end{array} \tag{8}$$

where l_1, l_2, m_1, and m_2 are positive constants that satisfy

$$m_1 < \phi_1 - \mu_1, m_2 < \phi_2 - \mu_2, l_1 < \varpi_1 - \kappa_1 - \varsigma_1, l_2 < \varpi_2 - \kappa_2 - \varsigma_2 \tag{9}$$

and $\zeta_1(0)$ and $\zeta_2(0)$ are selected, such that $|\zeta_1(0)| \leq m_1$ and $|\zeta_2(0)| \leq m_2$. (8) shows that $|\zeta_1(t)| \leq m_1$, $|\zeta_2(t)| \leq m_2$, $|\dot{\zeta}_1(t)| \leq l_1$, and $|\dot{\zeta}_2(t)| \leq l_2$ hold for all $t \geq 0$.

Dynamic Control Design: Define the velocity tracking error variables $\tilde{v} = v - \alpha_v$ and $\tilde{\omega} = \omega - \alpha_\omega$. Design the control torques as

$$\begin{array}{rcl} \tau_1 & = & -\varpi_1 \text{sign}(\tilde{v}) \\ \tau_2 & = & -\varpi_2 \text{sign}(\tilde{\omega}) \end{array} \tag{10}$$

where $\text{sign}(\cdot)$ denotes the standard signum function. It is pointed out that to implement the control law (7)–(10), all control parameters need only satisfy the condition (9). Therefore, they can be easily selected provided that the velocity and torque constraints (2) are provided.

For the convenience of notation, we define $c_0 = \mu_1 + \phi_1$, $c_1 = c_0 + 1$, $c_2 = c_1 + \mu_1^2 + \mu_2^2$, $c_3 = \phi_1 + \mu_1 + \phi_2$, $c_4 = \mu_2 + \phi_2$, $c_5 = \mu_1^2 + 2\mu_1\phi_1 + \phi_1^2 + \phi_1\phi_2 + \varpi_1 + \kappa_1 + \mu_1\mu_2 + (\mu_1 + \phi_1)$ c_0, $c_6 = 1 + 2c_0 + 2c_0^2 + c_5$, and $c_7 = 2\mu_1\kappa_1 + 2\mu_2\kappa_2 + (\mu_1^2 + \mu_2^2)(c_1 + c_2) + c_6$. Note that the parameters $c_0, c_1, \ldots, c_7$ are defined only for the control performance and are not used for the controller design. We are ready to state and prove the first main result of this paper.

Proposition 1. *Given any constraints $\phi_1 > 0$, $\phi_2 > 0$, $\varpi_1 > 0$, and $\varpi_2 > 0$ on the mobile robot (1) satisfying Assumption 1, we can always tune the design parameters in (7) and (10), such that the velocity and torque constraints given by (2) are never violated.*

Proof. For simplicity, the design parameters are chosen to satisfy

$$\lambda < \min\left\{ \frac{\phi_2 - \mu_2 - m_2}{\mu_1}, \frac{\varpi_2 - \kappa_2 - l_2 - \varsigma_2}{\kappa_1 + \mu_1(c_0 + c_3 + c_4)} \right\} \tag{11}$$

$$\rho < \min\left\{ \frac{\phi_2 - \mu_2 - m_2 - \lambda\mu_1}{c_2}, \frac{\varpi_1 - \kappa_1 - l_1 - \varsigma_1}{\mu_1 c_2}, \frac{\varpi_2 - \kappa_2 - l_2 - \varsigma_2 - \lambda(\kappa_1 + \mu_1(c_0 + c_3 + c_4))}{\lambda\mu_1 c_2 + c_7} \right\}. \tag{12}$$

We show that for any prespecified constants $\phi_1 > 0$, $\phi_2 > 0$, $\varpi_1 > 0$, and $\varpi_2 > 0$, the design parameters λ and ρ satisfying conditions (11) and (12) always exist. As m_2 and l_2 have been selected to satisfy $m_2 < \phi_2 - \mu_2$ and $l_2 < \varpi_2 - \kappa_2 - \varsigma_2$, there exists a positive λ, such that the condition (11) holds. This finding indicates that $\phi_2 - \mu_2 - m_2 - \lambda\mu_1 > 0$ and $\varpi_2 - \kappa_2 - l_2 - \varsigma_2 - \lambda(\kappa_1 + \mu_1(c_0 + c_3 + c_4)) > 0$. In addition, recalling (8) $l_1 < \varpi_1 - \kappa_1 - \varsigma_1$, we conclude that there exists a positive ρ, such that the condition (12) holds.

We now proceed to show that the velocity and torque constraints given by (2) under conditions (11) and (12) are never violated. As $|v_d(t)| \leq \mu_1$, it follows from (7) that $|\alpha_v(t)| \leq |v_d(t)| + |\zeta_1(t)| \leq \mu_1 + m_1 < \phi_1$. To prove $|v(t)| \leq \phi_1$, we consider $\dot{v}$ whenever $|v| = \phi_1$. Noting (10) and recalling $\phi_1 - \mu_1 - m_1 > 0$, we obtain:

$$\dot{v} = \begin{cases} -\varpi_1 + d_1, & \text{if } v = \phi_1 \\ \varpi_1 + d_1, & \text{if } v = -\phi_1 \end{cases}$$

As $|d_1(t)| < \varpi_1$ and $|v(0)| \leq \phi_1$, we conclude that $|v(t)| \leq \phi_1$ for all $t \geq 0$. Now, we prove that $|\omega(t)| \leq \phi_2$ for all $t \geq 0$. We need to examine the boundedness of $\dot{\xi}$ and α_ω. By direct computation, the time derivative of ξ is obtained as $\dot{\xi} = -(v_d^2 + \omega_d^2)\xi + \eta\dot{f}$, where $\dot{f}$ is given by

$$\dot{f} = \rho \sin t(1 - \tanh^2(\sqrt{1 + x_e^2 + y_e^2} - 1))\text{g} + \rho \cos t \tanh(\sqrt{1 + x_e^2 + y_e^2} - 1) \tag{13}$$

and $\text{g} = \frac{d(\sqrt{1+x_e^2+y_e^2})}{dt} = \frac{x_e(v - v_d\cos\theta_e) + y_e v_d \sin\theta_e}{\sqrt{1+x_e^2+y_e^2}}$. Noting $|y_e \sin\theta_e - x_e\cos\theta_e| \leq \sqrt{x_e^2 + y_e^2}$, we have $|\text{g}(t)| \leq |v_d(t)| + |v(t)| \leq c_0$, which, combined with (13), implies $|\dot{f}(t)| \leq \rho c_1$ and $|\dot{\xi}(t)| \leq \rho c_2$. Therefore, according to (7) and (12), we conclude that $|\alpha_\omega(t)| \leq \mu_2 + \lambda\mu_1 + m_2 + \rho c_2 < \phi_2$. Similar to the analysis of the boundedness of $v(t)$, we have $|\omega(t)| \leq \phi_2$ for all $t \geq 0$. In view of (10), we conclude that the constraints of τ_1 and τ_2 are guaranteed to be satisfied. □

The stability and asymptotic convergence of the closed-loop system composed of (1) and (10) are given by the following theorem.

Theorem 1. *Under Assumptions 1–3, by choosing the design parameter to satisfy (11) and (12), the control torque (10) forces the mobile robot (1) to globally asymptotically track the virtual robot (3) in the sense of (6).*

Proof. We first prove that $|\dot{\alpha}_v(t)| < \varpi_1 - \varsigma_1$ and $|\dot{\alpha}_\omega(t)| < \varpi_2 - \varsigma_2$ under the selection of (11) and (12). The time derivative of α_v is given by $\dot{\alpha}_v = \dot{v}_d \cos\xi - v_d\dot{\xi}\sin\xi - \dot{\zeta}_1$, which, combined with (12), indicates that $|\dot{\alpha}_v(t)| \le \kappa_1 + \rho\mu_1 c_2 + l_1 < \varpi_1 - \varsigma_1$. It can be obtained from (7) that

$$\dot{\alpha}_\omega = \ddot{\xi} + \dot{\omega}_d - \lambda\dot{v}_d\frac{x_e\sin\frac{\theta_e+\xi}{2} + y_e\cos\frac{\theta_e+\xi}{2}}{\sqrt{1+x_e^2+y_e^2}} - \lambda v_d\triangle - \dot{\zeta}_2 \tag{14}$$

where $\triangle = \triangle_1 + \triangle_2 + \triangle_3$ with

$$\triangle_1 = \frac{\dot{x}_e\sin\frac{\theta_e+\xi}{2} + \dot{y}_e\cos\frac{\theta_e+\xi}{2}}{\sqrt{1+x_e^2+y_e^2}}, \triangle_2 = \frac{(x_e\cos\frac{\theta_e+\xi}{2} - y_e\sin\frac{\theta_e+\xi}{2})(\dot{\theta}_e+\dot{\xi})}{\sqrt{1+x_e^2+y_e^2}}$$

$$\triangle_3 = -\frac{(x_e\sin\frac{\theta_e+\xi}{2} + y_e\cos\frac{\theta_e+\xi}{2})\mathrm{g}}{(1+x_e^2+y_e^2)}.$$

Noting $|-v_d\cos\theta_e\sin\frac{\theta_e+\xi}{2} + v_d\sin\theta_e\cos\frac{\theta_e+\xi}{2}| \le |v_d|$, we have $|\triangle_1(t)| \le |v(t)| + |v_d(t)| + |\omega(t)| \le c_3$, $|\triangle_2(t)| \le |\omega(t)| + |\omega_d(t)| + |\dot{\xi}(t)| \le c_4 + \rho c_2$, and $|\triangle_3(t)| \le |\mathrm{g}(t)| \le c_0$. Thus, we have $|\triangle(t)| \le \rho c_2 + c_0 + c_3 + c_4$. The second-order derivative of ξ is $\ddot{\xi} = -2(v_d\dot{v}_d + \omega_d\dot{\omega}_d)\xi - (v_d^2+\omega_d^2)(\dot{\xi}+\eta\dot{f}) + \eta\ddot{f}$, where

$$\begin{aligned}
\ddot{f} &= 2\rho\cos t(1-\tanh^2(\sqrt{1+x_e^2+y_e^2}-1))\mathrm{g} - \rho\sin t\tanh(\sqrt{1+x_e^2+y_e^2}-1)\\
&\quad -2\rho\sin t\tanh(\sqrt{1+x_e^2+y_e^2}-1)(1-\tanh^2(\sqrt{1+x_e^2+y_e^2}-1))\mathrm{g}^2\\
&\quad +\rho\sin t(1-\tanh^2(\sqrt{1+x_e^2+y_e^2}-1))h\\
h &= \frac{d^2(\sqrt{1+x_e^2+y_e^2})}{dt^2}\\
&= \frac{v_d^2 - 2v_dv\cos\theta_e + v^2 + \omega v y_e + x_e\tau_1 + \dot{v}_d(y_e\sin\theta_e - x_e\cos\theta_e)}{\sqrt{1+x_e^2+y_e^2}}\\
&\quad -\frac{(x_e\sin\theta_e + y_e\cos\theta_e)v_d\omega_d}{\sqrt{1+x_e^2+y_e^2}} - \frac{(x_e(v-v_d\cos\theta_e) + y_e v_d\sin\theta_e)\mathrm{g}}{1+x_e^2+y_e^2}.
\end{aligned}$$

Therefore, $|h(t)| \le c_5$, $|\ddot{f}(t)| \le \rho c_6$, and $|\ddot{\xi}(t)| \le \rho c_7$. By (12) and (14), we conclude that $|\dot{\alpha}_\omega(t)| \le \rho(c_7 + \lambda\mu_1 c_2) + \kappa_2 + \lambda\kappa_1 + \lambda\mu_1(c_0+c_3+c_4) + l_2 < \varpi_2 - \varsigma_2$.

The time derivatives of $\tilde{v}$ and $\tilde{\omega}$ are obtained as follows:

$$\begin{aligned}
\dot{\tilde{v}} &= -\varpi_1\mathrm{sign}(\tilde{v}) - \dot{\alpha}_v + d_1\\
\dot{\tilde{\omega}} &= -\varpi_2\mathrm{sign}(\tilde{v}) - \dot{\alpha}_\omega + d_2.
\end{aligned}$$

As $|-\dot{\alpha}_v(t) + d_1(t)| < \varpi_1$ and $|\dot{\alpha}_\omega(t) + d_2(t)| < \varpi_2$, by the sliding mode theory [33,34], there is a nonnegative constant T, such that $\tilde{v}(t) \equiv 0$ and $\tilde{\omega}(t) \equiv 0$ for $t \ge T$. Choosing $H = \frac{1}{2}\tilde{v}^2$ as a Lyapunov function candidate for $\dot{\tilde{v}} = -\varpi_1\mathrm{sign}(\tilde{v}) - \dot{\alpha}_v + d_1$, we obtain

$$\dot{H} = \tilde{v}(-\varpi_1\mathrm{sign}(\tilde{v}) - \dot{\alpha}_v + d_1) \le -\beta|\tilde{v}| \tag{15}$$

for some positive β. Thus, once the trajectory reaches the manifold $\tilde{v} = 0$, it cannot leave it. The invariance of $\tilde{\omega}$ can also be proven in a similar way. Consequently, the closed-loop error dynamics yield

$$\begin{array}{rcl} \dot{x}_e & = & v_d(\cos\xi - \cos\theta_e) + \omega y_e - \zeta_1 \\ \dot{y}_e & = & v_d \sin\theta_e - \omega x_e \\ \dot{\bar{\theta}}_e & = & -\frac{\lambda v_d}{\sqrt{1+x_e^2+y_e^2}}(x_e \sin\frac{\theta_e+\xi}{2} + y_e \cos\frac{\theta_e+\xi}{2}) - \zeta_2 \end{array} \tag{16}$$

where $\bar{\theta}_e = \theta_e - \xi$. The closed-loop stability and asymptotic convergence are analyzed using the following Lyapunov function candidate:

$$V = \sqrt{1+x_e^2+y_e^2} - 1 + \frac{4}{\lambda}(1 - \cos\frac{\bar{\theta}_e}{2}) + \frac{\zeta_1^2}{l_1} + \frac{2\zeta_2^2}{l_2\lambda} \tag{17}$$

whose derivative along (8) and (16) satisfies

$$\begin{array}{rcl} \dot{V} & = & \frac{x_e\dot{x}_e + y_e\dot{y}_e}{\sqrt{1+x_e^2+y_e^2}} + \frac{2}{\lambda}\dot{\bar{\theta}}_e \sin\frac{\bar{\theta}_e}{2} + \frac{2}{l_1}\zeta_1\dot{\zeta}_1 + \frac{4}{l_2\lambda}\zeta_2\dot{\zeta}_2 \\ & = & \frac{y_e v_d \sin\xi}{\sqrt{1+x_e^2+y_e^2}} - \frac{1}{m_1}\zeta_1^2 - \frac{1}{km_2}\zeta_2^2 \\ & \leq & |v_d \sin\xi| - \frac{1}{m_1}\zeta_1^2 - \frac{1}{km_2}\zeta_2^2. \end{array} \tag{18}$$

Note that the solution of η can be expressed as $\eta(t) = \exp(-\int_0^t (v_d^2(\sigma) + \omega_d^2(\sigma))d\sigma)$. A straightforward derivation shows that $0 < \exp(-\varepsilon_1) \leq \eta(t) \leq 1$ for case C1 and $\eta \in \mathcal{L}_1$ for case C2. By noting $|\sin(\xi)| \leq |\xi| \leq \rho\eta$, it can be verified that $v_d \sin\xi \in \mathcal{L}_1$ for both case C1 and case C2. Combined with (18), this result implies that $\zeta_1, \zeta_2 \in \mathcal{L}_2$ and $x_e, y_e, \zeta_1, \zeta_2 \in \mathcal{L}_\infty$. We further obtain from (8) that $\dot{\zeta}_1, \dot{\zeta}_2 \in \mathcal{L}_\infty$. Thus, the application of Barbalat's lemma leads to $\zeta_1, \zeta_2 \to 0$. Applying Lemma 1 to (8) yields $x_e, \sin\frac{\bar{\theta}_e}{2} \to 0$, which indicates $\bar{\theta}_e \to 2N\pi$, where N is an integer.

To this point, it remains to be proven that $y_e \to 0$. By Lemma 2, we conclude that $\dot{x}_e, \dot{\bar{\theta}}_e \to 0$, which combined with (16) implies $v_d(\cos\xi - \cos\theta_e) + \omega y_e, v_d y_e \cos\frac{\theta_e+\xi}{2} \to 0$. Noting

$$\cos\xi - \cos\theta_e = \sin\frac{\theta_e+\xi}{2}\sin\frac{\bar{\theta}_e}{2}, \cos\frac{\theta_e+\xi}{2} = \cos\frac{\bar{\theta}_e}{2}\cos\xi - \sin\frac{\bar{\theta}_e}{2}\sin\xi$$

we further obtain $\omega y_e, v_d y_e \cos\xi \to 0$. As $\tilde{v}(t) \equiv 0$ and $\tilde{\omega}(t) \equiv 0$ for all $t \geq T$, by noting (7), we have $(\dot{\xi} + \omega_d)y_e \to 0$. Recalling $\dot{\xi} = -(v_d^2 + \omega_d^2)\xi + \eta\dot{f}$, where $\dot{f}$ is given by

$$\dot{f} = \rho\sin t(1 - \tanh^2(\sqrt{1+x_e^2+y_e^2} - 1))\mathrm{g} + \rho\cos t\tanh(\sqrt{1+x_e^2+y_e^2} - 1)$$

with $\mathrm{g} = \frac{d(\sqrt{1+x_e^2+y_e^2})}{dt} = \frac{x_e(v - v_d\cos\theta_e) + y_e v_d \sin\theta_e}{\sqrt{1+x_e^2+y_e^2}}$, we separately analyze C1 and C2.

For case C1, as $\int_0^\infty (v_d^2(\sigma) + \omega_d^2(\sigma))d\sigma \leq \varepsilon_1$ and $v_d, \omega_d, \dot{v}_d, \dot{\omega}_d \in \mathcal{L}_\infty$, we have $v_d, \omega_d \to 0$. We obtain from $(\dot{\xi} + \omega_d)y_e \to 0$ that $\rho\eta\cos t\tanh(\sqrt{1+x_e^2+y_e^2} - 1)y_e \to 0$. This result coupled with $0 < \exp(-\varepsilon_1) \leq \eta(t)$ indicates that

$$\cos t\tanh(\sqrt{1+x_e^2+y_e^2} - 1)y_e \to 0.$$

From (18), we have $\frac{d(V - \int_0^t |v_d(\sigma)\sin\xi(\sigma)|d\sigma)}{dt} \leq 0$, implying that $V - \int_0^t |v_d(\sigma)\sin\xi(\sigma)|d\sigma$ is nonincreasing. Recalling

$$\int_0^t |v_d(\sigma)\sin\xi(\sigma)|d\sigma < \infty,$$

we conclude that $V(t)$ converges to a finite nonnegative constant. Therefore, we obtain from (17) that the limit of y_e exists and is finite. Therefore, we conclude that $y_e \to 0$ by simply seeking a contradiction.

For case C2, as $\int_t^{t+\varepsilon_3}(v_d^2(\sigma)+\omega_d^2(\sigma))d\sigma \geq \varepsilon_4$ and $\dot{f} \in \mathcal{L}_\infty$, we have $\eta, \xi, \dot{\xi} \to 0$. Thus, we have $w_d y_e, v_d y_e \to 0$, which indicates $(|w_d|+|v_d|)y_e \to 0$. It is straightforward to show that $y_e \to 0$.

It follows from $x_e, y_e \to 0$ that $f \to 0$. Thus, we have $\xi \to 0$ for both case C1 and case C2. We conclude that $\theta_e - \bar{\theta}_e \to 0$. Here, we complete the proof. □

Remark 5. *Compared with recent research on nonholonomic mobile robots [10,11,13–15], our proposed method has several clear advantages. First, most of these studies necessitate either a nonzero reference linear velocity or a nonzero reference angular velocity. Therefore, these findings may not be directly applicable to the stabilization problem. In contrast, our developed unified controller does not impose such a requirement. Second, none of these studies take into account velocity or torque constraints. Our controller, however, ensures that predefined constraints (2) are always satisfied.*

Remark 6. *Numerous techniques have been proposed for nonholonomic systems with input saturation, including passivity- and normalization-based methods [19], adaptive schemes [28], dynamic feedback methods [35], and switching control strategies [21]. However, most of these studies focus on either velocity saturation or control torque saturation. In contrast, our work considers both velocity and control torque constraints (2). Furthermore, unlike separated saturation control strategies for stabilization and tracking tasks in [19,28], this paper introduces a unified tracking and stabilization control controller for nonholonomic mobile robots. These two distinctive features set our work apart from existing methods for nonholonomic systems with input saturation.*

Remark 7. *This work focuses on the stabilization and tracking control problem of single mobile robots. There are currently some interesting results [36,37], where formation control algorithms for multiple unmanned surface vehicles were presented using reinforcement learning methods. Unlike the asymptotic convergence of the tracking error achieved in this work, these studies obtained optimality and uniformly ultimately bounded stability. Combining our results with the techniques in [36,37] is an important research direction.*

4. Comparative Simulations and Validations

In this section, we conduct extensive simulations to illustrate the application of our method. The objective is to make the robot (1) track the virtual robot (3) under the following velocity and torque constraints:

$$|v(t)| \leq 1.6 \text{ m/s}, |\omega(t)| \leq 5.1 \text{ rad/s}, |\tau_1(t)| \leq 3.3 \text{ N} \cdot \text{m}, |\tau_2(t)| \leq 51 \text{ N} \cdot \text{m}.$$

The constraints of the reference trajectory are $\mu_1 = 0.5$ m/s, $\mu_2 = 0.2$ rad/s, $\kappa_1 = 1$ N· m, and $\kappa_2 = 1$ N· m, which satisfy Assumption 2. For simplicity, we choose $d_1(t) = 0$ and $d_2(t) = 0$. The control parameters given in Table 1 are selected according to (8), (10), (11), and (12). In the following part, we will consider the tracking task and stabilization task to illustrate the performance of our unified controller.

Table 1. Control parameters.

Parameter	m_1	m_2	l_1	l_2	λ	ρ
Value	0.5	0.5	0.5	0.5	1	1

Tracking Task. By Assumption 3, the virtual robot defined by (3) runs along a circle with $v_d = 0.5$ m/s and $\omega_d = 0.2$ rad/s. The simulation results are shown in Figures 2–6. Although the robot is subject to nonholonomic constraints and the initial tracking error is relatively large, Figure 2 shows that the robot controlled by our proposed adaptive control torque (10) converges to the reference trajectory asymptotically. The trajectories of the resulting velocity and the required torque are depicted in Figures 3–6, respectively, with their constraints plotted as red dashed lines. It is clear that the robot's velocity and control torque remain within the prespecified range at all times, as analyzed in Proposition 1.

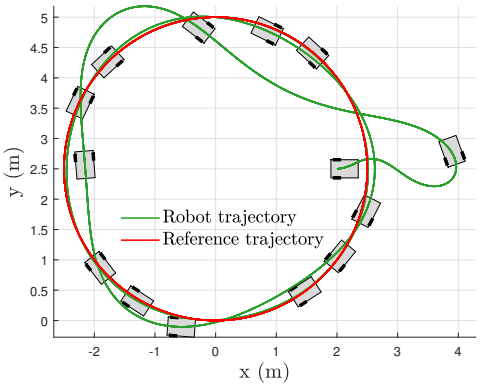


Figure 2. Tracking task: robot position in the (X,Y) plane.

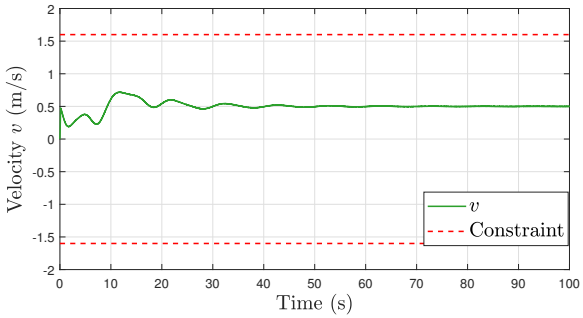


Figure 3. Tracking task: the resulting linear velocity v and its constraints.

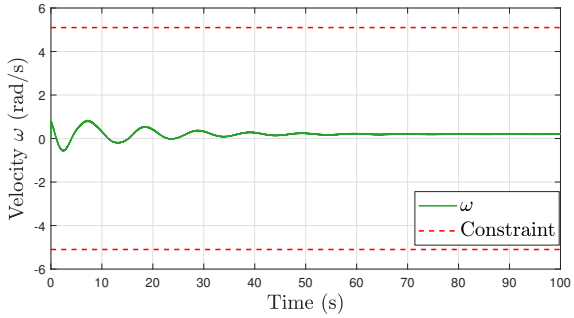


Figure 4. Tracking task: the resulting angular velocity ω and its constraints.

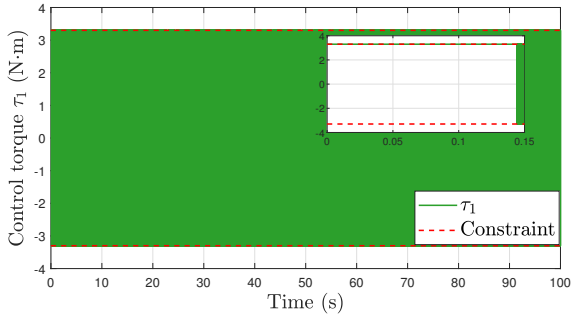


Figure 5. Tracking task: the required control torque τ_1 and its constraints.

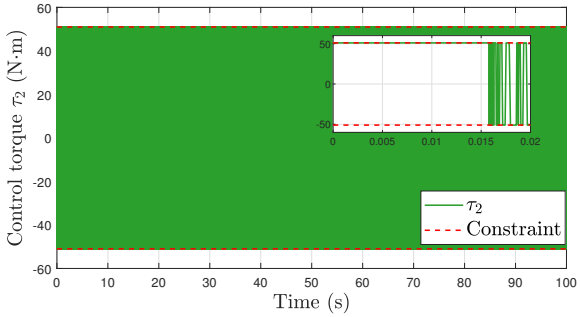


Figure 6. Tracking task: the required control torque τ_2 and its constraints.

Stabilization Task. Based on Assumption 3, we set $v_d = 0$ m/s and $\omega_d = 0$ rad/s. The simulation results are shown in Figures 7–11. Figure 7 illustrates the behavior of the robot's position and orientation over time. The graph clearly shows that both the position and orientation of the robot asymptotically converge to their respective reference values. Figures 8–11 provide a comprehensive view of the trajectories for the robot's linear velocity v, angular velocity ω, and the torques τ_1 and τ_2 required for movement. The constraints imposed on these variables are visually represented by red dashed lines in their graphs. These constraints are defined as $|v(t)| \leq 1.6$ m/s, $|\omega(t)| \leq 5.1$ rad/s, $|\tau_1(t)| \leq 3.3$ N · m, and $|\tau_2(t)| \leq 51$ N · m. The plots clearly show that at no point on the trajectories of v, ω, τ_1, or τ_2 exceed these prescribed limits. This observation confirms the effectiveness of our proposed method.

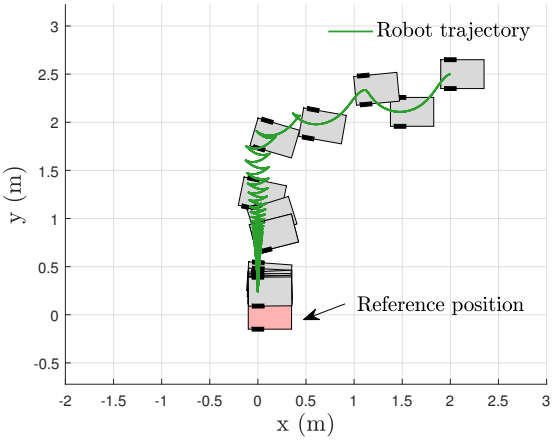


Figure 7. Stabilization task: robot position in the (X,Y) plane.

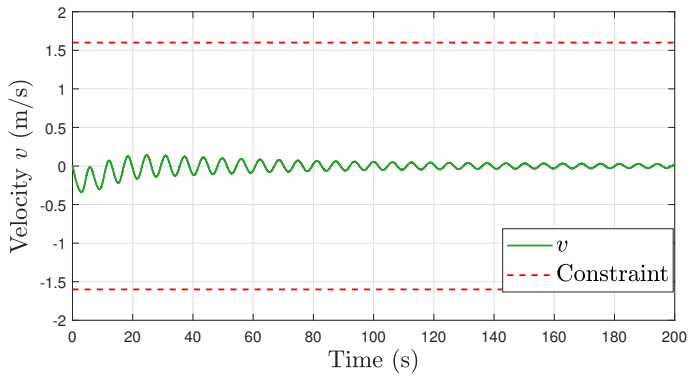


Figure 8. Stabilization task: the resulting linear velocity v and its constraints.

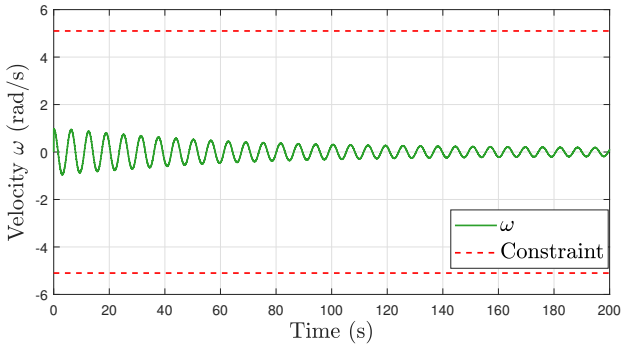


Figure 9. Stabilization task: the resulting angular velocity ω and its constraints.

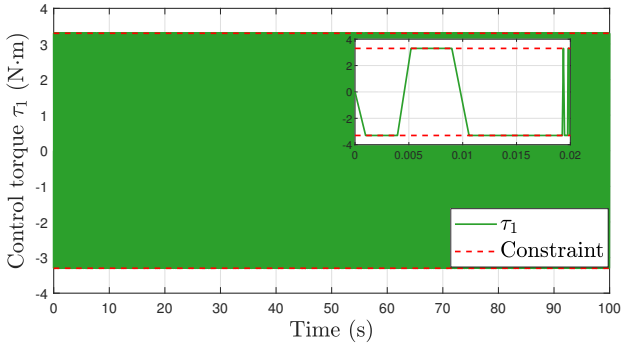


Figure 10. Stabilization task: the required control torque τ_1 and its constraints.

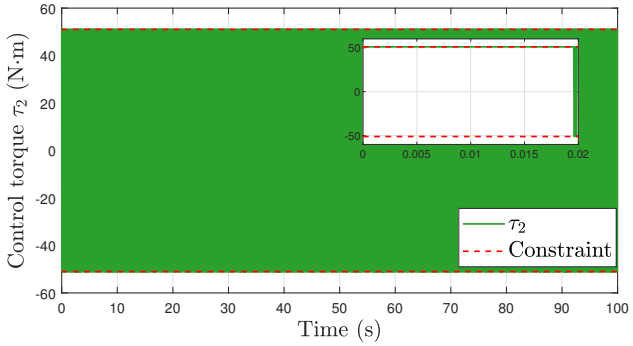


Figure 11. Stabilization task: the required control torque τ_2 and its constraints.

Chattering Reduction. The controllers (10) employ a signum function to ensure finite-time convergence of $\tilde{v}$ and $\tilde{w}$. However, this approach may lead to chattering in the application. To eliminate chattering, we can replace the signum function with a continuous boundary layer function as

$$\tau_1 = \begin{cases} -\varpi_1 \text{sign}(\tilde{v}), & \text{if } \tilde{v} \geq \epsilon_1 \\ -(\varpi_1 \tilde{v})/\epsilon_1, & \text{if } \tilde{v} < \epsilon_1 \end{cases}, \tau_2 = \begin{cases} -\varpi_2 \text{sign}(\tilde{\omega}), & \text{if } \tilde{\omega} \geq \epsilon_2 \\ -(\varpi_2 \tilde{\omega})/\epsilon_2, & \text{if } \tilde{\omega} < \epsilon_2 \end{cases} \tag{19}$$

where ϵ_1 and ϵ_2 are small positive constants. These modifications still ensure the satisfaction of the velocity and torque constraints. The stabilization and tracking errors do not achieve asymptotic convergence, but rather converge to a residual set, the size of which may depend on the adjustable parameters ϵ_1 and ϵ_2 (a rigorous proof necessitates further investigation). This aspect is not the focus of this work. The simulation results of the tracking task are shown in Figures 12–14 to illustrate this situation; all control parameters are the same as in the tracking task, except that (19) with $\epsilon_1 = 0.1$ and $\epsilon_2 = 0.1$ is applied.

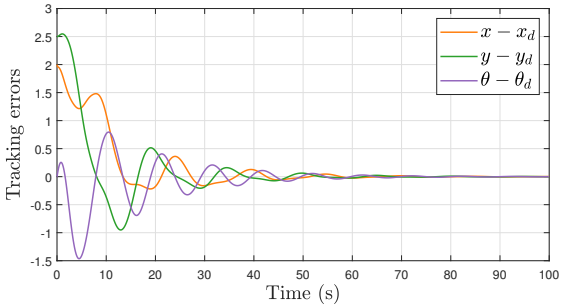


Figure 12. Chattering reduction: position and orientation tracking errors with (19).

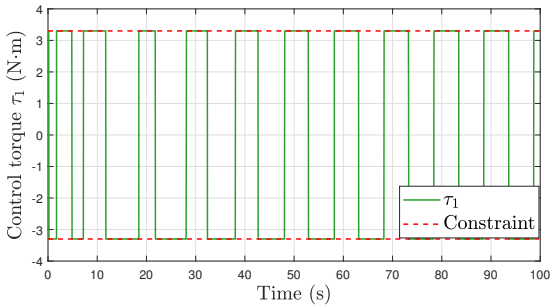


Figure 13. Chattering reduction: the required control torque τ_1 with (19).

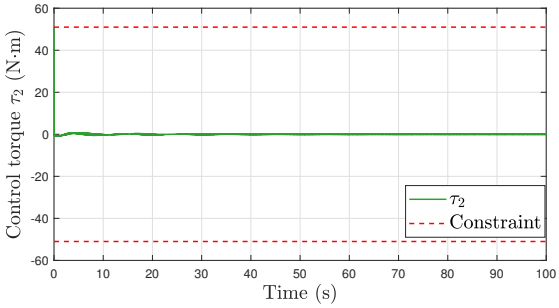


Figure 14. Chattering reduction: the required control torque τ_2 with (19).

Comparative Simulations. We conduct two comparative simulations using the classical control methods for nonholonomic mobile robots under the same initial conditions. In particular, the first simulation employs a tracking approach that does not consider velocity constraints [7], while the second simulation uses separated saturated stabilization and tracking control strategies [19]. The control parameters in [7] are chosen as $c_1 = 7$ and $c_2 = 0.1$. The reference trajectory is the same as in the tracking task described above. The simulation results are shown in Figures 15–17. Although asymptotic tracking control is obtained by [7], it can be seen from Figure 16 that the robot velocity constraint is violated.

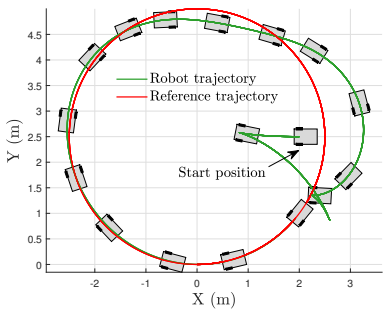


Figure 15. Tracking task: robot position in the (X,Y) plane with the tracking approach in [7].

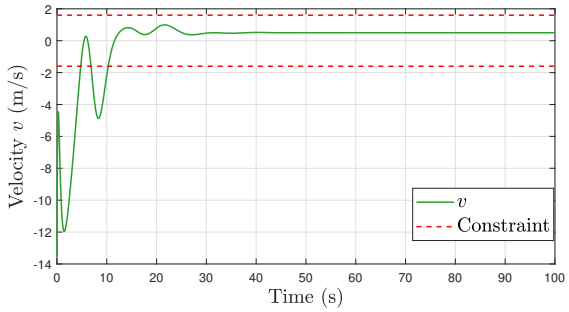


Figure 16. Tracking task: the required linear velocity v and its constraints with the tracking approach in [7].

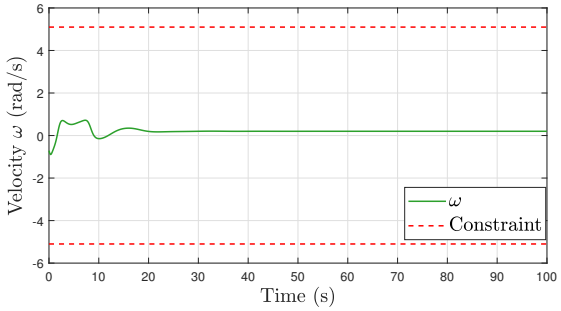


Figure 17. Tracking task: the required angular velocity ω and its constraints with the tracking approach in [7].

To demonstrate the improved transient performance of the robot velocity by our proposed controller, as compared to using the separated saturated controllers in [19], a reference trajectory that consists of a time-varying trajectory for the initial 70 s and a stationary point for the remaining duration is selected. Specifically, the time-varying trajectory is defined by (3) with $v_d = 0.5$ m/s and $\omega_d = 0.2$ rad/s, while the stationary point is selected as $(x_d, y_d, \theta_d) = (0, 0, 0)$. The control parameters in [19] are chosen as $\varepsilon_1 = 1.6$, $\varepsilon_2 = 4$, and $\varepsilon_3 = 1$ for the stabilization task and $\lambda_1 = 4.5$, $\lambda_2 = 0.4$, and $\lambda_3 = 1.1$ for the tracking task. For our proposed controller, the control parameters in Table 1 are utilized. Simulation results in Figures 18–20 demonstrate that both the separated controllers in [19] and our proposed controller can achieve satisfactory trajectory tracking and stabilization within the velocity constraints. Note from Figure 19 that at 70 s, the linear velocity v under the controllers in [19] exhibits a rapid oscillation. This oscillation is induced by the transition from the tracking controller to the stabilization controller. However, given the unified properties of our proposed controller for both tracking and stabilization control tasks, such an impact is absent. These results substantiate that our unified controller can improve the transient performance of robot velocity.

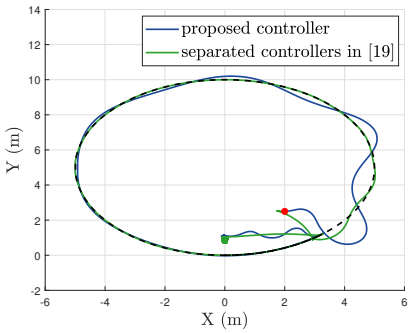


Figure 18. Comparative simulation: robot position in the (X,Y) plane.

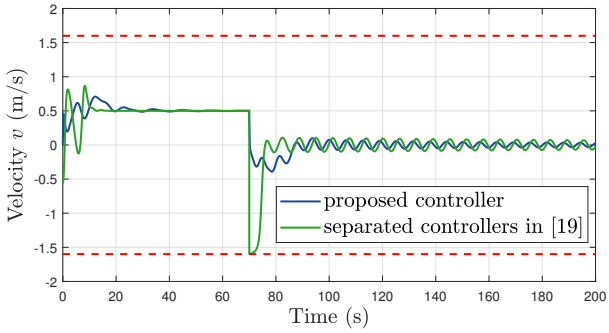


Figure 19. Comparative simulation: the linear velocity v and its constraints.

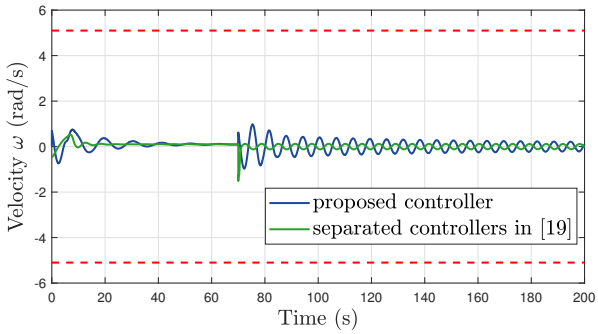


Figure 20. Comparative simulation: the angular velocity ω and its constraints.

5. Conclusions and Future Work

Despite the uncertainties in the dynamic model, a new unified controller has been developed to address the tracking and stabilization of nonholonomic mobile robots. Theoretical analysis and extensive simulations have been presented to demonstrate that asymptotic tracking and stabilization can be achieved and that all closed-loop signals remain bounded under the proposed controller. One of the salient properties of the proposed method is that it can ensure that the prescribed velocity and torque constraints are not transgressed by simply choosing the design parameter a priori. Ongoing work extends our proposed approach by addressing more realistic scenarios such as general disturbances and nonlinearities in the wheels of a mobile robot.

Author Contributions: Methodology, Y.L.; Investigation, W.L.; Formal analysis, Y.L.; Writing—original draft, G.W.; Writing—review and editing, Y.W.; Validation, Y.C.; Project administration, W.L. All authors have read and agreed to the published version of the manuscript.

Funding: This research was funded by the Natural Science Foundation of Shanghai under Grant 22ZR1443600.

Data Availability Statement: Data are contained within the article.

Conflicts of Interest: The authors declare no conflicts of interest.

References

1. Wu, Y.; Zhao, Y.; Yu, J. Global asymptotic stability controller of uncertain nonholonomic systems. *J. Frankl. Inst.* **2013**, *350*, 1248–1263. [CrossRef]
2. Dixon, W.E.; Jiang, Z.P.; Dawson, D.M. Global exponential setpoint control of wheeled mobile robots: A Lyapunov approach. *Automatica* **2000**, *36*, 1741–1746. [CrossRef]
3. Yu, J.; Liu, Y.; Wu, Y. Output feedback stabilization for nonholonomic systems with unknown unmeasured states-dependent growth. *Int. J. Robust Nonlinear Control* **2020**, *30*, 1788–1801. [CrossRef]
4. Sánchez-Torres, J.D.; Defoort, M.; Muñoz-Vázquez, A.J. Predefined-time stabilisation of a class of nonholonomic systems. *Int. J. Control* **2020**, *93*, 2941–2948. [CrossRef]

5. Hou, D.; Gao, F.; Huang, J.; Wu, Y. A switching-based state-scaling design for prescribed-time stabilization of nonholonomic systems with actuator dead-zones. *Aerosp. Sci. Technol.* **2021**, *118*, 106986. [CrossRef]
6. Canudas de Wit, C.; Siciliano, B.; Bastin, G. *Theory of Robot Control*; Springer Science & Business Media: London, UK, 2012.
7. Jiang, Z.P.; Nijmeijer, H. Tracking control of mobile robots: A case study in backstepping. *Automatica* **1997**, *33*, 1393–1399.
8. Yang, F.; Wang, C.; Jing, G. Adaptive tracking control for dynamic nonholonomic mobile robots with uncalibrated visual parameters. *Int. J. Adapt. Control Signal Process.* **2013**, *27*, 688–700. [CrossRef]
9. Zhai, J.; Song, Z. Adaptive sliding mode trajectory tracking control for wheeled mobile robots. *Int. J. Control* **2019**, *92*, 2255–2262. [CrossRef]
10. Ou, M.; Sun, H.; Zhang, Z.; Gu, S. Fixed-time trajectory tracking control for nonholonomic mobile robot based on visual servoing. *Nonlinear Dyn.* **2022**, *108*, 251–263. [CrossRef]
11. Lin, L.; Xu, Z.; Zheng, J. Predefined Time Active Disturbance Rejection for Nonholonomic Mobile Robots. *Mathematics* **2023**, *11*, 2704. [CrossRef]
12. Meng, H.; Zhang, J.; Li, S. Dual-mode robust model predictive control for the tracking control of nonholonomic mobile robot. *Int. J. Robust Nonlinear Control* **2023**, *33*, 3627–3639. [CrossRef]
13. Yan, L.; Ma, B.; Jia, Y. Trajectory tracking control of nonholonomic wheeled mobile robots using only measurements for position and velocity. *Automatica* **2024**, *159*, 111374. [CrossRef]
14. Pliego-Jiménez, J.; Martínez-Clark, R.; Cruz-Hernández, C.; Arellano-Delgado, A. Trajectory tracking of wheeled mobile robots using only Cartesian position measurements. *Automatica* **2021**, *133*, 109756. [CrossRef]
15. Cui, M.; Liu, H.; Wang, X.; Liu, W. Adaptive control for simultaneous tracking and stabilization of wheeled mobile robot with uncertainties. *J. Intell. Robot. Syst.* **2023**, *108*, 46. [CrossRef]
16. Do, K.D.; Jiang, Z.P.; Pan, J. Simultaneous tracking and stabilization of mobile robots: An adaptive approach. *IEEE Trans. Autom. Control* **2004**, *49*, 1147–1151. [CrossRef]
17. Wang, Y.; Miao, Z.; Zhong, H.; Pan, Q. Simultaneous stabilization and tracking of nonholonomic mobile robots: A Lyapunov-based approach. *IEEE Trans. Control Syst. Technol.* **2015**, *23*, 1440–1450. [CrossRef]
18. Li, B.; Fang, Y.; Hu, G.; Zhang, X. Model-free unified tracking and regulation visual servoing of wheeled mobile robots. *IEEE Trans. Control Syst. Technol.* **2016**, *24*, 1328–1339. [CrossRef]
19. Jiang, Z.P.; Lefeber, E.; Nijmeijer, H. Saturated stabilization and tracking of a nonholonomic mobile robot. *Syst. Control Lett.* **2001**, *42*, 327–332. [CrossRef]
20. Wang, C. Semiglobal practical stabilization of nonholonomic wheeled mobile robots with saturated inputs. *Automatica* **2008**, *44*, 816–822. [CrossRef]
21. Gao, F.; Yuan, Y.; Wu, Y. Finite-time stabilization for a class of nonholonomic feedforward systems subject to inputs saturation. *Isa Trans.* **2016**, *64*, 193–201. [CrossRef]
22. Chen, X.; Jia, Y.; Matsuno, F. Tracking control for differential-drive mobile robots with diamond-shaped input constraints. *IEEE Trans. Control Syst. Technol.* **2014**, *22*, 1999–2006. [CrossRef]
23. Chen, X.; Jia, Y. Simple tracking controller for unicycle-type mobile robots with velocity and torque constraints. *Trans. Inst. Meas. Control* **2015**, *37*, 211–218. [CrossRef]
24. Yu, X.; Liu, L.; Feng, G. Trajectory tracking for nonholonomic vehicles with velocity constraints. *IFAC—PapersOnLine* **2015**, *48*, 918–923. [CrossRef]
25. Hu, J.; Zhang, Y.; Rakheja, S. Adaptive Trajectory Tracking for Car-like Vehicles with Input Constraints. *IEEE Trans. Ind. Electron.* **2022**, *69*, 2801–2810. [CrossRef]
26. Lee, T.C.; Song, K.T.; Lee, C.H.; Teng, C.C. Tracking control of unicycle-modeled mobile robots using a saturation feedback controller. *IEEE Trans. Control Syst. Technol.* **2001**, *9*, 305–318.
27. Wang, Z.; Li, G.; Chen, X.; Zhang, H.; Chen, Q. Simultaneous stabilization and tracking of nonholonomic WMRs with input constraints: Controller design and experimental validation. *IEEE Trans. Ind. Electron.* **2019**, *66*, 5343–5352. [CrossRef]
28. Huang, J.; Wen, C.; Wang, W.; Jiang, Z.P. Adaptive stabilization and tracking control of a nonholonomic mobile robot with input saturation and disturbance. *Syst. Control Lett.* **2013**, *62*, 234–241. [CrossRef]
29. Li, J.W. Adaptive Tracking and Stabilization of Nonholonomic Mobile Robots With Input Saturation. *IEEE Trans. Autom. Control* **2022**, *67*, 6173–6179. [CrossRef]
30. Sira-Ramirez, H.; Agrawal, S.K. *Differentially Flat Systems*; CRC Press: New York, NY, USA, 2018.
31. Wang, G. Consensus algorithm for multi-agent systems with nonuniform communication delays and its application to nonholonomic robot rendezvous. *IEEE Trans. Control Netw. Syst.* **2023**, *10*, 1496–1507. [CrossRef]
32. Slotine, J.J.E.; Li, W. *Applied Nonlinear Control*; Prentice Hall: Upper Saddle River, NJ, USA, 1991.
33. Utkin, V.I. Sliding mode control design principles and applications to electric drives. *IEEE Trans. Ind. Electron.* **1993**, *40*, 23–36. [CrossRef]
34. Utkin, V.I. *Sliding Modes in Control and Optimization*; Springer: New York, NY, USA, 2013.
35. Chen, H.; Wang, C.; Zhang, B.; Zhang, D. Saturated tracking control for nonholonomic mobile robots with dynamic feedback. *Trans. Inst. Meas. Control* **2013**, *35*, 105–116. [CrossRef]

36. Nguyen, K.; Dang, V.T.; Pham, D.D.; Dao, P.N. Formation control scheme with reinforcement learning strategy for a group of multiple surface vehicles. *Int. J. Robust Nonlinear Control* **2024**, *34*, 2252–2279. [CrossRef]
37. Chen, L.; Dong, C.; He, S.; Dai, S.L. Adaptive optimal formation control for unmanned surface vehicles with guaranteed performance using actor-critic learning architecture. *Int. J. Robust Nonlinear Control* **2023**, *33*, 4504–4522. [CrossRef]

Disclaimer/Publisher's Note: The statements, opinions and data contained in all publications are solely those of the individual author(s) and contributor(s) and not of MDPI and/or the editor(s). MDPI and/or the editor(s) disclaim responsibility for any injury to people or property resulting from any ideas, methods, instructions or products referred to in the content.